

Performances of non-dissipative structure-dependent integration methods

Shuenn-Yih Chang*

Department of Civil Engineering, National Taipei University of Technology,
1, Section 3, Jungshiau East Road, Taipei 106-08, Republic of China

(Received July 23, 2017, Revised October 4, 2017, Accepted October 7, 2017)

Abstract. Three structure-dependent integration methods with no numerical dissipation have been successfully developed for time integration. Although these three integration methods generally have the same numerical properties, such as unconditional stability, second-order accuracy, explicit formulation, no overshoot and no numerical damping, there still exist some different numerical properties. It is found that TLM can only have unconditional stability for linear elastic and stiffness softening systems for zero viscous damping while for nonzero viscous damping it only has unconditional stability for linear elastic systems. Whereas, both CEM and CRM can have unconditional stability for linear elastic and stiffness softening systems for both zero and nonzero viscous damping. However, the most significantly different property among the three integration methods is a weak instability. In fact, both CRM and TLM have a weak instability, which will lead to an adverse overshoot or even a numerical instability in the high frequency responses to nonzero initial conditions. Whereas, CEM possesses no such an adverse weak instability. As a result, the performance of CEM is much better than for CRM and TLM. Notice that a weak instability property of CRM and TLM might severely limit its practical applications.

Keywords: weak instability; numerical instability; overshoot; structure-dependent integration method

1. Introduction

An unconditionally stable, explicit structure-dependent integration method was first proposed by Chang to overcome the difficulty experienced in the pseudo-dynamic test (2002), where a test specimen with high frequency modes cannot be conducted due to numerical explosions for explicit pseudo-dynamic algorithm. Although an implicit pseudo-dynamic algorithm can have unconditional stability it is very complex to be implemented for an actual pseudo-dynamic test due to the involvement of an iteration procedure. In addition to the applications to conduct pseudo-dynamic tests, it is also found that a structure-dependent integration method is promising for a nonlinear dynamic analysis since it simultaneously has unconditional stability and explicit formulation. Hence, it is computationally efficient for solving a structural dynamics problem, where the total solution is dominated by the low frequency modes while high frequency responses are of no interest. Consequently, many structure-dependent integration methods were developed subsequently (Chang 2007, 2009, 2010, 2014a, b, c, 2015a, Chang *et al.* 2015, 2016, Chen and Ricles 2008, Gui *et al.* 2014, Kolay and Ricles 2014, 2016, Mohammadzadeh *et al.* 2017, Tang and Lou 2017).

In a conventional integration method (Newmark 1959, Hilber *et al.* 1977, Wood *et al.* 1981, Chung and Hulbert 1993, Fung 2001, 2002, Civalek 2007, Krenk 2008, Gao, *et al.* 2012, Hadianfard 2012, Alamatian 2013), the coefficients

of the displacement and velocity difference equations are scalar constants while for a structure-dependent integration method, its coefficients of the two difference equations are no longer limited to be scalar constants but can be functions of the initial structural properties and the step size. Hence, this type of integration methods is classified as structure-dependent integration methods. It is well recognized that an unconditional stability property is important for a structure-dependent integration method. However, it is generally found that a structure-dependent integration method can only have unconditional stability for the stiffness softening and linear elastic systems while for the stiffness hardening systems it only has a conditional stability. (Chang 2007, 2009, 2010, 2014a, b, c, 2015a, Chang *et al.* 2015, 2016, Chen and Ricles 2008, Gui *et al.* 2014, Kolay and Ricles 2014, 2016). In order to overcome this adverse property, a stability amplification factor has been applied to enlarge the unconditional stability range (Chang 2015b). This technique seems applicable to a general structure-dependent integration method and thus the stability properties can be significantly improved.

There are three structure-dependent integration methods among the currently available integration methods. It can be shown that these three integration methods can have the same characteristic equation for an undamped linear elastic system and thus it will lead to exactly the same numerical properties. However, their performances might be significantly different in solving some specific structural dynamics problems. The first Chang explicit method (CEM) is published in 2002 and is a member of the first Chang family method (2010). The CR explicit method (CRM) is a special member of the second Chang family method (2014a). In the near recent, an explicit structure-dependent

*Corresponding author, Professor
E-mail: changsy@ntut.edu.tw

integration method was proposed by Tang and Lou in 2017 for a real-time pseudo-dynamic test. It will be referred as TL method (TLM) for brevity herein. In general, the major differences among the three integration methods are the different difference equations, either scalar or structure-dependent coefficients as well as either explicit or implicit form. It is of great interest to examine these three integration methods and to determine the one that can have the best performance for the nonlinear dynamic analysis. For this purpose, the numerical properties of the three integration methods are summarized first. Next, the adverse properties, such as the stability property for nonzero viscous damping, weak instability and an overshoot in a high frequency steady-state response are explored and compared.

2. General formulation

The general formulation of CEM, CRM and TLM can be simply expressed as

$$\begin{aligned} ma_{i+1} + cv_{i+1} + kd_{i+1} &= f_{i+1} \\ d_{i+1} &= d_i + \beta_1(\Delta t)v_i + \beta_2(\Delta t)^2 a_i \\ v_{i+1} &= v_i + \gamma_1(\Delta t)a_i + \gamma_2(\Delta t)a_{i+1} \end{aligned} \quad (1)$$

where d_i , v_i , a_i and f_i are the displacement, velocity, acceleration and external force at the i -th time step, respectively. The coefficients of β_1 , β_2 , γ_1 and γ_2 for CEM, CRM and TLM are found to be:

$$\begin{cases} \beta_1 = \frac{1}{D}(1 + \xi\Omega_0) \\ \beta_2 = \frac{1}{D} \end{cases} \quad \begin{cases} \gamma_1 = \frac{1}{2} \\ \gamma_2 = \frac{1}{2} \end{cases} \quad \text{CEM} \\ \begin{cases} \beta_1 = 1 \\ \beta_2 = \frac{1}{D} \end{cases} \quad \begin{cases} \gamma_1 = \frac{1}{D} \\ \gamma_2 = 0 \end{cases} \quad \text{CRM} \\ \begin{cases} \beta_1 = \frac{1}{D} \\ \beta_2 = \frac{1}{D}[1 - \xi\Omega_0 - \xi^2] \end{cases} \quad \begin{cases} \gamma_1 = 1 \\ \gamma_2 = 0 \end{cases} \quad \text{TLM} \end{cases} \quad (2)$$

where $\Omega_0 = \omega_0(\Delta t)$ and $\omega_0 = \sqrt{k_0/m}$ is an initial natural frequency, where k_0 is the initial stiffness; ξ is a viscous damping ratio. In addition, $D = 1 + \xi\Omega_0 + \frac{1}{4}\Omega_0^2$ is defined.

Clearly, the three integration methods all have an explicit, structure-dependent displacement difference equation while their velocity difference equations are drastically different. An implicit form with scalar coefficients is found for CEM while CRM has an explicit form with structure-dependent coefficients. Finally, TLM possesses an explicit form with scalar coefficients. It is evident that these three integration methods are significantly different in the formulations.

3. Numerical properties of linear elastic systems

Since the basic analysis of each integration method has

been explored before, it will not be conducted herein again. However, the basic numerical properties are summarized for comparison. For this purpose, the characteristic equation for zero viscous damping and for a linear elastic system is

$$\lambda \left[\lambda^2 - 2 \left(\frac{1 - \frac{1}{4}\Omega_0^2}{1 + \frac{1}{4}\Omega_0^2} \right) \lambda + 1 \right] = 0 \quad (3)$$

where λ is an eigenvalue of the characteristic equation. It can be found that this equation is exactly the same as that of the constant average acceleration method (AAM). Hence, the stability, period distortion and numerical damping properties for CEM, CRM and TLM will be exactly the same as those of AAM.

Since an overshoot in the early high frequency transient response has been found by Goudreau and Taylor in 1972 for the Wilson- θ method (Wilson 1968) and it cannot be detected by means of assessing the characteristic equation, a simple technique has been proposed by Hilber and Hughes in 1978 to detect such an unusual overshoot behavior. A tendency to overshoot the exact solution of an integration method can be revealed by calculating the free vibration response to a single degree of freedom system for the current time step subject to the initial conditions of the previous step data as $\Omega_0 \rightarrow \infty$. As a result, the results for CEM, CRM and TLM for the limiting cases of $\Omega_0 \rightarrow \infty$ are found to be

$$\begin{cases} d_{i+1} \approx -d_i \\ v_{i+1} \approx -v_i \end{cases} \quad \text{CEM} \\ \begin{cases} d_{i+1} \approx -3d_i + (\Delta t)v_i \\ v_{i+1} \approx -4 \left(\frac{d_i}{\Delta t} \right) + v_i \end{cases} \quad \text{CRM} \\ \begin{cases} d_{i+1} \approx -3d_i \\ v_{i+1} \approx \left(\frac{d_i}{\Delta t} \right) + v_i \end{cases} \quad \text{TLM} \end{cases} \quad (4)$$

This equation reveals that there is no overshooting behavior in displacement and velocity for CEM, CRM and TLM since each term is independent of Ω_0 .

In order to confirm the overshoot behaviors of the three integration methods, the displacement and velocity

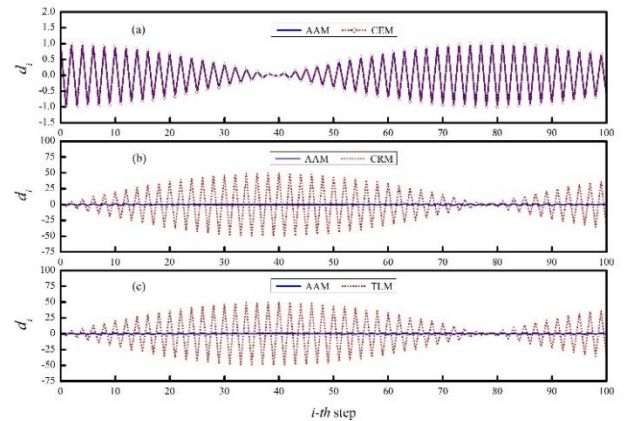


Fig. 1 Comparison of overshoot in displacement response

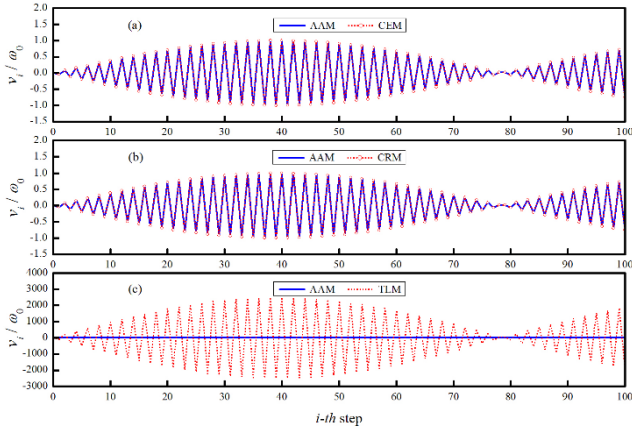


Fig. 2 Comparison of overshoot in velocity response

responses are calculated by using CEM, CRM and TLM. The initial conditions of $d_0=1$ and $v_0=1$ are taken. A time step of $\Delta t=10T_0$ is adopted. The velocity term is normalized by the initial natural frequency of the system in order to have the same unit as displacement. Calculated results are shown in Figs. 1 and 2 for the displacement and velocity responses, respectively. In Fig. 1(a), the calculated results obtained from CEM are exactly the same as those obtained from AAM and exhibit no overshoot in displacement. On the other hand, it is manifested from Figs. 1(b) and 1(c) that the results obtained from CRM and TLM largely overshoot the results obtained from AAM and show a significant overshoot. It is seen that the velocity responses obtained from CEM and CRM are the same as those obtained from AAM and involve no overshoot in velocity as shown in Figs. 2(a) and 2(b). Meanwhile, in Fig. 2(c), the results obtained from TLM clearly exhibits a very significant overshoot behavior. It is evident that the overshoot behaviors found in displacement and velocity for CRM and TLM are inconsistent with the analytical results shown in Eq. (4). Hence, the cause of this inconsistency must be further explored.

4. Weak instability

In order to figure out the root cause of the inconsistency between the calculated results shown in Figs. 1 and 2 and the analytical results shown in Eq. (4), an analytical scheme is applied to derive the numerical solution, which is obtained from each integration method, in a mathematical form. Thus, the free vibration response of an undamped, linear elastic single degree of freedom system is calculated by using CEM, CRM and TLM. Hence, the equation of motion with a zero dynamic loading is considered. The initial conditions of the initial displacement of d_0 and the initial velocity of v_0 are adopted. Clearly, a theoretical solution for this problem can be simply obtained from the fundamental theory of structural dynamics for comparison purpose and is found to be

$$d_n = \cos(n\Omega_0)d_0 + \frac{\sin(n\Omega_0)}{\Omega_0}(\Delta t)v_0 \quad (5)$$

where $d_n=u(t_n)$ and $t_n=n(\Delta t)$.

In general, the step-by-step integration procedure for the use of an integration method to solve a dynamic problem can be written in a recursive matrix form (Belytschko and Hughes 1983, Su and Xu 2014) and is

$$\mathbf{X}_n = \mathbf{A}\mathbf{X}_{n-1} = \mathbf{A}^2\mathbf{X}_{n-2} = \dots = \mathbf{A}^n\mathbf{X}_0 \quad (6)$$

where $\mathbf{X}_n=[d_n, (\Delta t)v_n, (\Delta t)^2 a_n]^T$ is defined and the case of $n=0$ implies $\mathbf{X}_0=[d_0, (\Delta t)v_0, (\Delta t)^2 a_0]^T$. Thus, for the initial conditions of d_0 and v_0 , the initial acceleration a_0 can be determined from the equation of motion and is $(\Delta t)^2 a_0 = -2\zeta\Omega_0(\Delta t)v_0 - \Omega_0^2 d_0$ for a free vibration response. If there exist three linearly independent eigenvectors for the amplification matrix, Eq. (6) can further reduce to be

$$\mathbf{X}_n = \mathbf{A}^n\mathbf{X}_0 = \mathbf{\Phi}\mathbf{\Lambda}^n\mathbf{\Phi}^{-1}\mathbf{X}_0 \quad (7)$$

where $\mathbf{\Lambda}$ is a diagonal matrix and its diagonal term λ_i , for $i=1,2,3$, is an eigenvalue of the matrix \mathbf{A} ; $\mathbf{\Phi}$ is an eigenvector matrix and each column ϕ_i , for $i=1,2,3$, is the eigenvector corresponding to λ_i . In general, they can be explicitly expressed as:

$$\mathbf{\Lambda} = \begin{bmatrix} \lambda_1 & 0 & 0 \\ 0 & \lambda_2 & 0 \\ 0 & 0 & \lambda_3 \end{bmatrix}, \quad \mathbf{\Phi} = [\phi_1 \quad \phi_2 \quad \phi_3] \quad (8)$$

On the other hand, an amplification matrix \mathbf{A} may not be diagonalized for an integration method if it is lack of three linearly independent eigenvectors. In this case, Eq. (7) is not applicable. However, there will exist a non-singular matrix $\mathbf{\Psi}$ to transform the matrix \mathbf{A} into a Jordan canonical form such as $\mathbf{A}=\mathbf{\Psi}\mathbf{J}\mathbf{\Psi}^{-1}$, where \mathbf{J} is the Jordan form of the matrix \mathbf{A} . As a result, Eq. (7) can be rewritten as

$$\mathbf{X}_n = \mathbf{A}^n\mathbf{X}_0 = \mathbf{\Psi}\mathbf{J}^n\mathbf{\Psi}^{-1}\mathbf{X}_0 \quad (9)$$

Hence, the following equation can be achieved

$$\mathbf{J} = \begin{bmatrix} \lambda & 1 & 0 \\ 0 & \lambda & 1 \\ 0 & 0 & 0 \end{bmatrix}, \quad \mathbf{\Psi} = [\psi_1 \quad \psi_2 \quad \psi_3] \quad (10)$$

if the amplification matrix \mathbf{A} has a double root in addition to a zero root. Thus, there exist no three linearly independent eigenvectors. As a result, either Eq. (7) or (9) can be directly applied to derive the numerical solution in a mathematical form.

Based on Eq. (3), the three eigenvalues for CEM, CRM and TLM can be simply determined from Eq. (3) and are found to be

$$\lambda_{1,2} = \frac{1 - \frac{1}{4}\Omega_0^2}{1 + \frac{1}{4}\Omega_0^2} \pm i \frac{\Omega_0}{1 + \frac{1}{4}\Omega_0^2}, \quad \lambda_3 = 0 \quad (11)$$

In addition, the corresponding eigenvector matrix for CEM is found to be

$$\mathbf{\Phi}_{CEM} = \begin{bmatrix} 1 & 1 & \frac{1}{4}\alpha^2\Omega_0^2 \\ i\Omega_0 & -i\Omega_0 & \frac{1}{2}\alpha(1 - \frac{1}{4}\Omega_0^2) \\ -\Omega_0^2 & -\Omega_0^2 & -1 \end{bmatrix} \quad (12)$$

where

$$\alpha = \frac{1}{1 + \frac{1}{4}\Omega_0^2} \quad (13)$$

Similarly, for CRM, it is found to be

$$\Phi_{CRM} = \begin{bmatrix} 1 & 1 & 0 \\ \frac{1}{2}\alpha\Omega_0^2 + i\alpha\Omega_0 & \frac{1}{2}\alpha\Omega_0^2 - i\alpha\Omega_0 & \alpha \\ -\Omega_0^2 & -\Omega_0^2 & -1 \end{bmatrix} \quad (14)$$

Finally, for TLM, it is found to be

$$\Phi_{TLM} = \begin{bmatrix} 1 & 1 & 0 \\ \frac{1}{2}\Omega_0^2 + i\Omega_0 & \frac{1}{2}\Omega_0^2 - i\Omega_0 & 1 \\ -\Omega_0^2 & -\Omega_0^2 & -1 \end{bmatrix} \quad (15)$$

Eqs. (12), (14) and (15) reveal that CEM, CRM and TLM, in general, can have three linearly independent eigenvectors for a general value of Ω_0 . Hence, Eq. (7) can be used to obtain the numerical solution in a mathematical form for the three integration methods and it is found to be

$$d_n = \cos(n\bar{\Omega}_0) d_0 + \frac{\sin(n\bar{\Omega}_0)}{\Omega_0} (\Delta t) v_0 \quad (16)$$

where $\bar{\Omega}_0 = \cos^{-1} \left[\left(1 - \frac{1}{4}\Omega_0^2 \right) / \left(1 + \frac{1}{4}\Omega_0^2 \right) \right]$ is found and it is a calculated value corresponding to a true value Ω_0 . Eq. (16) reveals that there is no overshoot for a general Ω_0 .

Since an overshoot was found in the high frequency free vibration responses for CRM and TLM, it is of great interest to obtain the numerical solution in a mathematical form in the limit $\Omega_0 \rightarrow \infty$. Notice that the eigenvector matrices for CEM, CRM and TLM in the limit $\Omega_0 \rightarrow \infty$ will become

$$\begin{aligned} \Phi_{CEM} &= \begin{bmatrix} 1 & 1 & 0 \\ i\Omega_0 & -i\Omega_0 & -2 \\ -\Omega_0^2 & -\Omega_0^2 & -1 \end{bmatrix} \\ \Phi_{CRM} &= \begin{bmatrix} 1 & 1 & 0 \\ 2 & 2 & 0 \\ -\Omega_0^2 & -\Omega_0^2 & 1 \end{bmatrix} \\ \Phi_{TLM} &= \begin{bmatrix} 0 & 0 & 0 \\ 1 & 1 & 1 \\ -2 & -2 & -1 \end{bmatrix} \end{aligned} \quad (17)$$

It is important to note that CEM can still have three linearly independent eigenvectors. As a result, it will also lead to the solution in Eq. (16) in the limiting case of $\Omega_0 \rightarrow \infty$. On the other hand, $\phi_1 = \phi_2$ for CRM and TLM as $\Omega_0 \rightarrow \infty$. In this case, Eq. (9) can be applied to mathematically derive the numerical solution for using CRM and TLM. Hence, it is of need to derive Ψ and \mathbf{J} at first. As a result, they are found to be

$$\Psi_{CRM} = \begin{bmatrix} 1 & 0 & 0 \\ 2 & 1 & 0 \\ -\Omega_0^2 & 0 & 1 \end{bmatrix}, \quad \mathbf{J}_{CRM} = \begin{bmatrix} -1 & 1 & 0 \\ 0 & -1 & 0 \\ 0 & 0 & 0 \end{bmatrix} \quad (18)$$

Table 1 Comparisons of coefficients for d_0 and $(\Delta t)v_0$

Method	Coefficient of d_0	Coefficient of $(\Delta t)v_0$
Exact Solution	$\cos(n\Omega_0)$	$\frac{\sin(n\Omega_0)}{\Omega_0}$
CEM	$\cos(n\bar{\Omega}_0)$	$\frac{\sin(n\bar{\Omega}_0)}{\Omega_0}$
CRM	$(2n+1)(-1)^n$	$-n(-1)^n$
TLM	$(2n+1)(-1)^n$	$\frac{\sin(n\bar{\Omega}_0)}{\Omega_0}$

for CRM. Whereas, for TLM, Ψ_{TLM} and \mathbf{J}_{TLM} can be also derived by using the same procedure and are found to be

$$\Psi_{TLM} = \begin{bmatrix} 2 & 1 & 0 \\ \Omega_0^2 & \Omega_0^2 & 1 \\ -2\Omega_0^2 & -\Omega_0^2 & -1 \end{bmatrix}, \quad \mathbf{J}_{TLM} = \begin{bmatrix} -1 & 1 & 0 \\ 0 & -1 & 0 \\ 0 & 0 & 0 \end{bmatrix} \quad (19)$$

Subsequently, the term \mathbf{J}^n in Eq. (9) can be obtained after a simple calculation and the result is found to be

$$\mathbf{J}_{CRM}^n = \mathbf{J}_{TLM}^n = \begin{bmatrix} (-1)^n & n(-1)^{n-1} & 0 \\ 0 & (-1)^n & 0 \\ 0 & 0 & 0 \end{bmatrix} \quad (20)$$

where an upper off-diagonal term of the matrix is nonzero. Substituting Eqs. (19) and (20) into Eq. (9), the numerical solutions of d_n in mathematical forms for CRM and TLM in the limit $\Omega_0 \rightarrow \infty$ are found to be

$$\begin{aligned} d_n &= (2n+1)(-1)^n d_0 - n(-1)^n (\Delta t) v_0 & \text{CRM} \\ d_n &= (2n+1)(-1)^n d_0 + \frac{\sin(n\bar{\Omega}_0)}{\Omega_0} (\Delta t) v_0 & \text{TLM} \end{aligned} \quad (21)$$

Next, the mathematically obtained numerical solutions can be compared to the theoretical solution for each integration method for discussing the overshoot behaviors found in Figs. 1 and 2.

For the convenience of the subsequent comparison study, the coefficients of the theoretical and numerical solutions are summarized in Table 1.

After comparing Eqs. (16) to (5), it is seen that the numerical solution obtained from CEM in the limit $\Omega_0 \rightarrow \infty$ is almost the same as the theoretical solution except for the very slight difference between the true Ω_0 and the calculated $\bar{\Omega}_0$ in a numerical procedure. Thus, there is no weak instability for CEM. Consequently, CEM exhibits no overshooting both in displacement and velocity in Figs. 1 and 2. Meanwhile, it is seen that the numerical solution obtained from CRM is very different from the theoretical solution. In addition, the coefficients of d_0 and $(\Delta t)v_0$ increase with the increase of the number of n . Notice that the coefficient of d_0 for the exact solution is $\cos(n\Omega_0)$, which is varied from -1 to 1 ; and that for $(\Delta t)v_0$ is $\sin(n\Omega_0)/\Omega_0$, which diminishes to zero for a large Ω_0 . Thus, the difference between Eq. (5) and the first line of equation (21) will become significant for a large Ω_0 . In fact, the coefficients of d_0 and $(\Delta t)v_0$ reveal that CRM experiences a weak instability for high frequency modes.

Since the coefficient of d_0 for TLM is the same as that of CRM and thus TLM also has a weak instability for nonzero initial displacement. Notice that the coefficient of $(\Delta t)v_0$ for TLM is the same as that of CEM and thus TLM has no weak instability for nonzero initial velocity.

Clearly, the phenomena found in Figs. 1 and 2 can be thoroughly explained by the analytical results. Since CEM has no weak instability, it exhibits no overshoot. Whereas, the overshoot behaviors found in high frequency responses for CRM and TLM are caused by weak instability. Hence, the inconsistency between the analytical predictions of Eq. (4) and the overshoot behaviors found in Figs. 1 and 2 can be resolved. As a result, the overshooting behaviors found in Figs. 1 and 2 originate from a weak instability property but not the overshoot behavior found by Goudreau and Taylor.

5. Overshoot under dynamic loading

It is evident from Eq. (4) that there is no overshoot both in displacement and velocity in the free vibration response obtained from CEM, CRM and TLM. However, a different overshoot has been found in the high frequency steady-state response if a general structure-dependent integration method is adopted to conduct time integration (Chang *et al.* 2016). In fact, the cause of this overshoot and its remedy for CEM and CRM have been shown in the above reference and will not be elaborated here again. However, those of TLM are still not explored.

To show an overshoot in the high frequency steady-state response, the following example is considered.

$$m\ddot{u}(t) + k_0 u(t) = k_0 \sin(\bar{\omega}t) \quad (22)$$

where $\bar{\omega}$ is the applied frequency of the sine loading. The theoretical solution of this equation can be directly derived from the fundamental theory of structural dynamics (Penzien 2004) and is found to be

$$u(t) = \frac{1}{1-\beta^2} \sin(\bar{\omega}t) - \frac{\beta}{1-\beta^2} \sin(\omega_0 t) \quad (23)$$

where $\beta = \bar{\omega} / \omega_0$ is a frequency ratio. In order to focus on the steady-state response, a small β value will be adopted for numerical illustrations since it implies a low frequency mode. Hence, in the limiting case of $\beta \rightarrow 0$ or for a small β , Eq. (23) is approximated by $u(t) \approx \sin(\bar{\omega}t)$. This case can be achieved by taking $m=1$, $k_0=10^8$ and $\bar{\omega}=0.5$. As a result, the natural frequency of the system is found to be 10^4 rad/sec and the value of $\beta=5 \times 10^{-5}$ is found. A time step of $\Delta t=1$ sec is chosen to calculate the response for the zero initial conditions by employing CEM, CRM and TLM. Numerical results are plotted in Fig. 3. It is expected that an accurate solution can be obtained if the steady-state response is reliably integrated. It has been shown by Chang (2006) that a harmonic load can be faithfully represented if a time step is chosen to satisfy $\Delta t / \bar{T} \leq \frac{1}{12}$, where \bar{T} is the period of the harmonic load. For this case, the value of $\Delta t / \bar{T} = \frac{1}{4\pi} \leq \frac{1}{12}$ implies that the applied sine load can be accurately captured and a reliable steady-state result can be

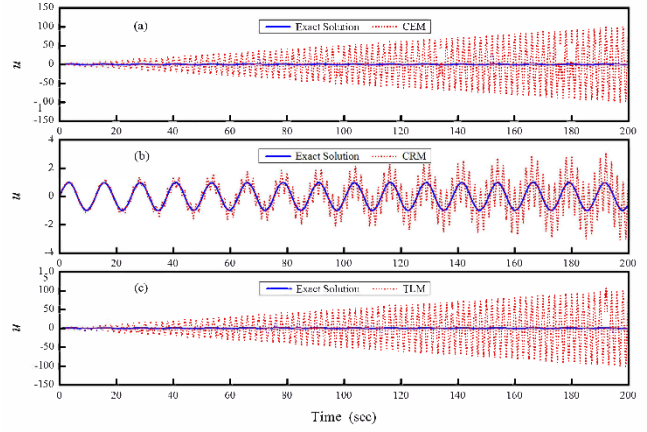


Fig. 3 Displacement responses to dynamic loading for using CEM, CRM and TLM

obtained. However, a very significant overshoot is found in Fig. 3 for CEM, CRM and TLM. The cause of this overshoot for CEM and CRM have been explored by Chang *et al.* (2016) and is due to the lack of a load-dependent term in the displacement difference equation. However, it is still not studied for TLM. Since the same procedure is used to explore TLM, only the analytical results are presented here in addition to CEM and CRM for comparison.

The cause of the overshoot under dynamic loading can be revealed by a local truncation error constructed from a forced vibration response. As a result, the local truncation errors for the three integration methods for zero viscous damping are found to be

$$\begin{aligned} E_{CEM} &= \frac{1}{D} \left[\frac{1}{4} \Omega_0^2 \ddot{u}_i + \frac{1}{3} \xi \Omega_0 (\Delta t) \dddot{u}_i + \frac{1}{12} (\Delta t)^2 \ddot{u}_i \right] \\ &\quad + \frac{1}{BD} \frac{1}{2m} \xi \Omega_0 (\Delta t) \left[\dot{f}_i - \frac{1}{2} (\Delta t) \ddot{f}_i \right] + O[(\Delta t)^3] \\ E_{CRM} &= \frac{1}{D} \left[\frac{1}{4} \Omega_0^2 \ddot{u}_i + \frac{1}{3} \xi \Omega_0 (\Delta t) \ddot{u}_i + \frac{1}{12} (\Delta t)^2 \ddot{u}_i \right] \\ &\quad + O[(\Delta t)^3] \end{aligned} \quad (24)$$

$$\begin{aligned} E_{TLM} &= \frac{1}{D} \left[\frac{1}{4} \Omega_0^2 \ddot{u}_i + \frac{1}{3} \xi \Omega_0 (\Delta t) \ddot{u}_i + \frac{1}{12} (\Delta t)^2 \ddot{u}_i \right] \\ &\quad + \frac{1}{D} \frac{1}{m} \left(\frac{1}{2} \xi \Omega + 2\xi^2 \right) (\Delta t) \left[\dot{f}_i - \frac{1}{2} (\Delta t) \ddot{f}_i \right] + O[(\Delta t)^3] \end{aligned}$$

where $B=1+\xi\Omega_0$. This equation reveals that CEM, CRM and TLM have a second-order accuracy. It is also found that the local truncation error of each integration method will be controlled by the term $\frac{1}{4}\Omega_0^2\ddot{u}_i/D$ for high frequency modes since it is quadratically proportional to Ω_0 .

After exploring the root cause of this type of overshoot, it is very important to propose a remedy to eliminate it. For this purpose, a load-dependent term is introduced into the displacement difference equation to cancel out the dominant error term $\frac{1}{4}\Omega_0^2\ddot{u}_i/D$. In general, the second line of Eq. (1) is modified to be

$$d_{i+1} = d_i + \beta_1 (\Delta t) v_i + \beta_2 (\Delta t)^2 a_i + p_{i+1} \quad (25)$$

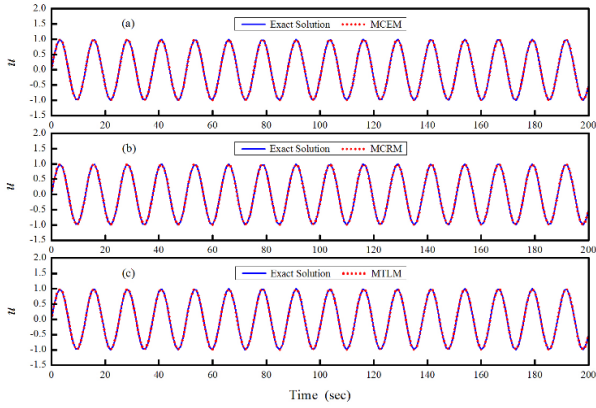


Fig. 4 Displacement responses to dynamic loading for using MCEM, MCRM and MTLM

where p_{i+1} is a load-dependent term. Hence, CEM, CRM and TLM will be referred as MCEM, MCRM and MTLM after this modification of displacement difference equation. The load-dependent term can be determined from the local truncation error of each modified integration method (Chang *et al.* 2016). As a result, the load-dependent term for each integration method is found to be the same and is

$$p_{i+1} = \frac{1}{D} \frac{1}{4m} (\Delta t)^2 (f_{i+1} - f_i) \quad (26)$$

where f_{i+1} and f_i are the loading terms defined in Eq. (1) in correspondence to the $(i+1)$ -th and i -th time step. After adding p_{i+1} into the displacement difference equation for each integration method, the dominant error term for each integration method can be automatically eliminated. Hence, the overshoot behavior in the high frequency steady-state response can be removed. To confirm the effectiveness of this load-dependent term, Eq. (22) is solved again by using these three integration methods and the results are shown in Fig. 4. Apparently, the calculated results obtained from MCEM, MCRM and MTLM are almost coincided together with the exact solution. Hence, it is strongly recommended that the load-dependent term must be included in the formulation of a structure-dependent integration method so that there will be no overshoot in a high frequency steady-state response.

6. Nonlinear stability property

Although the numerical properties of CEM, CRM and TLM for a linear elastic system are well studied and summarized in the previous sections it is very important to examine their actual performances in the step by step solution of a nonlinear system. A parameter called the instantaneous degree of nonlinearity has been proposed by Chang (2007) to monitor the stiffness change for a nonlinear system. It is generally defined as the ratio of the stiffness at the end of the i -th time step over the initial stiffness and is

$$\delta_i = \frac{k_i}{k_0} \quad (27)$$

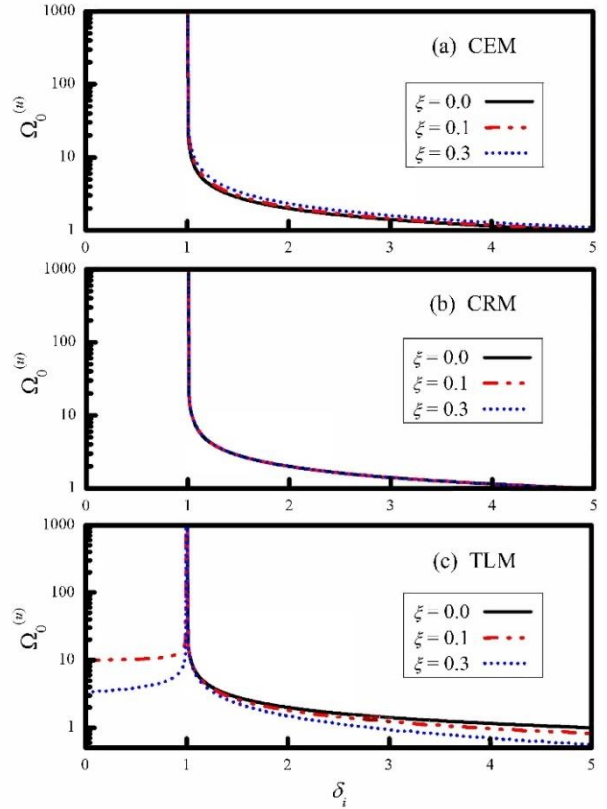


Fig. 5 Variation of upper stability limit with δ_i

Clearly, $\delta_i=1$ implies that the instantaneous stiffness at the end of the i -th time step is equal to the initial stiffness. Whereas, $\delta_i>1$ denotes stiffness hardening and the instantaneous stiffness is larger than the initial stiffness at the end of the i -th time step; $0<\delta_i<1$ is used to represent a stiffness softening case, where the instantaneous stiffness is less than the initial stiffness.

To assess the stability property of CEM, CRM and TLM for a linear elastic system, it is of great interest to look into the variation of the upper stability limit $\Omega_0^{(u)}$ with the instantaneous degree of nonlinearity δ_i for a different viscous damping ratio as shown in Fig. 5. Clearly, for zero viscous damping, these three integration methods have an unconditional stability in the range of $\delta_i \leq 1$ while they can only have a conditional stability in the range of $\delta_i > 1$. It is also found that the variation of the upper stability property is generally unaffected by a nonzero viscous damping ratio for CEM and CRM. Whereas, it is highly affected by a nonzero viscous damping ratio for TLM. In fact, TLM can only have an unconditional stability as $\delta_i=1$ for a nonzero viscous damping ratio. In other words, for a nonzero viscous damping ratio, TLM can only have an unconditional stability for linear elastic systems.

7. Numerical example

In the following numerical illustrations, a 5-story shear-beam type building, as shown in Fig. 6, is applied to confirm the properties of a weak instability and an

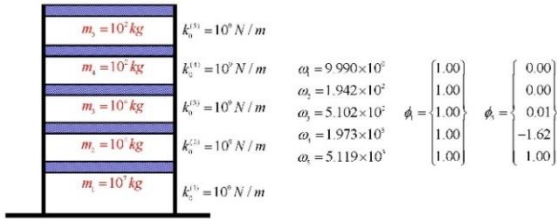


Fig. 6 Structural and vibrational properties of a 5-story shear-beam building

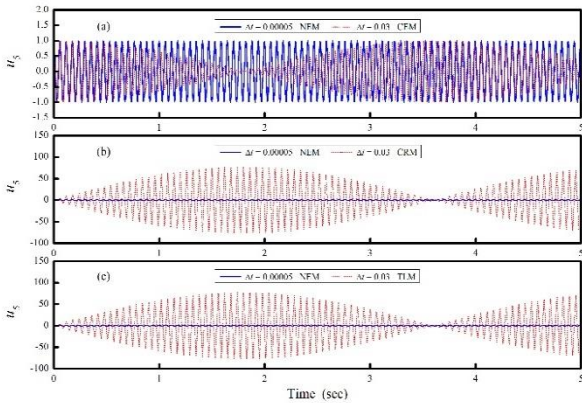


Fig. 7 Free vibration responses at top floor for a 5-story building

overshoot in a high frequency steady-state response for a linear elastic, multiple degree of freedom system for CEM, CRM and TLM.

The lowest and highest natural frequencies of the building are found to be 9.99 and 5.12×10^3 rad/sec, respectively.

At first, free vibration responses to the initial condition of $\mathbf{u}(0)=\phi_5$ is considered. The numerical result obtained from NEM with $\Delta t=5 \times 10^{-5}$ sec is treated as a reference solution. This time step is small enough to accurately integrate the fifth mode since the value of $\Delta t/T_0$ is as small as 0.041 for this mode. Meanwhile, a time step of $\Delta t=0.03$ sec is also used to compute the responses for CEM, CRM and TLM. The calculated results at the top floor are plotted in Fig. 7.

Although CEM is unable to achieve an accurate solution due to the use of a relatively large time step, it clearly exhibits no amplitude growth effect in the response. However, a very significant amplitude growth was found in the responses obtained from CRM and TLM. The root cause of this drastic difference is because that CEM has no weak instability while CRM and TLM have an adverse weak instability property.

Next, a sine loading is applied at the top story and it is $f(t)=10^8 \sin(5\pi t)N$. The solutions are calculated by using the time step of $\Delta t=0.03$ sec for CEM, CRM and TLM and their corresponding modified methods. This problem is also solved by using NEM with $\Delta t=5 \times 10^{-5}$ sec and this result is considered as a reference solution for comparison. All the results are plotted in Fig. 8.

It is manifested from Figs. 8(a) to 8(c) that CEM, CRM and TLM exhibit an overshoot in the forced vibration

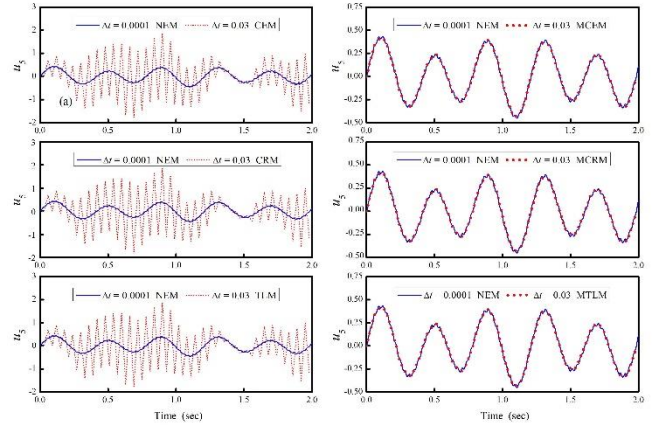


Fig. 8 Top story responses of 5-story building under a sine load at top floor

Table 2 Comparison of numerical properties

Property	CEM	CRM	TLM
Unconditional stability	Yes	Yes	No
Second-order accuracy	Yes	Yes	Yes
Explicit formulation	Yes	Yes	Yes
Controllable numerical damping	No	No	No
Overshoot in transient response	No	No	No
Overshoot in steady-state response	Yes	Yes	Yes
Weak instability	No	Yes	Yes

response. On the other hand, it is seen in Figs. 8(d) to 8(f) that MCEM, MCRM and TLM can give very accurate solutions. Notice that $\Delta t=0.03$ sec is small enough to faithfully represent the sine loading since the value of $\Delta t/T_0$ is as small as 0.075. These results validate that CEM, CRM and TLM will generally lead to an adverse overshoot in a high frequency steady-state response while this adverse overshoot can be effectively eliminated by introducing an appropriate load-dependent term into the displacement difference equation.

8. Conclusions

As a summary of this comparative study, the major numerical properties of the three integration methods are summarized in Table 2. In general, the numerical properties, such as the stability, a second-order accuracy, an overshoot in transient response and zero numerical damping, are exactly the same for a linear elastic system for the three integration methods. It is found that each integration method has an overshoot in the high frequency steady-state response and this overshoot can be eliminated by adding a load-dependent term into its displacement difference equation. Notice that TLM is shown to be only conditionally stable for a nonzero viscous damping ratio for any nonlinear systems.

The most detrimental property to CRM and TLM is a weak instability or overshoot in the high frequency

responses to nonzero initial conditions. This implies that the numerical solutions obtained from either CRM or TLM may experience an overshoot or even numerical instability for nonzero initial conditions. This is a very stringent limitation and therefore its practical applications might be of no interest. It is evident that the root cause of this weak instability is due to the three linearly dependent eigenvectors for high frequency modes and thus the amplification matrix cannot be diagonalized. On the other hand, CEM can still have three linearly independent eigenvectors for high frequency modes and therefore its amplification matrix is diagonalizable. As a result, it has no adverse weak instability property or overshooting. Hence, CEM is strongly recommended for practical applications among the three integration methods.

Acknowledgments

The author is grateful to acknowledge that this study is financially supported by the National Science Council, Taiwan, R.O.C., under Grant No.NSC-105-2221-E-027-029.

References

- Alamatian, J. (2013), "New implicit higher order time integration for dynamic analysis", *Struct. Eng. Mech.*, **48**(5), 711-736.
- Belytschko, T. and Hughes, T.J.R. (1983), *Computational Methods for Transient Analysis*, Elsevier Science Publishers B.V., North-Holland, Amsterdam.
- Chang, S.Y. (2002), "Explicit pseudodynamic algorithm with unconditional stability", *J. Eng. Mech.*, ASCE, **128**(9), 935-947.
- Chang, S.Y. (2006), "Accurate representation of external force in time history analysis", *J. Eng. Mech.*, ASCE, **132**(1), 34-45.
- Chang, S.Y. (2007), "Improved explicit method for structural dynamics", *J. Eng. Mech.*, ASCE, **133**(7), 748-760.
- Chang, S.Y. (2009), "An explicit method with improved stability property", *Int. J. Numer. Meth. Eng.*, **77**(8), 1100-1120.
- Chang, S.Y. (2010), "A new family of explicit method for linear structural dynamics", *Comput. Struct.*, **88**(11-12), 755-772.
- Chang, S.Y. (2014a), "Family of structure-dependent explicit methods for structural dynamics", *J. Eng. Mech.*, ASCE, **140**(6), 06014005.
- Chang, S.Y. (2014b), "Numerical dissipation for explicit, unconditionally stable time integration methods", *Earthq. Struct.*, **7**(2), 157-176.
- Chang, S.Y. (2014c), "A family of non-iterative integration methods with desired numerical dissipation", *Int. J. Numer. Meth. Eng.*, **100**(1), 62-86.
- Chang, S.Y. (2015a), "Dissipative, non-iterative integration algorithms with unconditional stability for mildly nonlinear structural dynamics", *Nonlin. Dyn.*, **79**(2), 1625-1649.
- Chang, S.Y. (2015b), "A general technique to improve stability property for a structure-dependent integration method", *Int. J. Numer. Meth. Eng.*, **101**(9), 653-669.
- Chang, S.Y., Wu, T.H. and Tran, N.C. (2015), "A family of dissipative structure-dependent integration methods", *Struct. Eng. Mech.*, **55**(4), 815-837.
- Chang, S.Y., Wu, T.H. and Tran, N.C. (2016), "Improved formulation for a structure-dependent integration method", *Struct. Eng. Mech.*, **60**(1), 149-162.
- Chen, C. and Ricles, J.M. (2008), "Development of direct integration algorithms for structural dynamics using discrete control theory", *J. Eng. Mech.*, ASCE, **134**(8), 676-683.
- Chung, J. and Hulbert, G.M. (1993), "A time integration algorithm for structural dynamics with improved numerical dissipation: the generalized- α method", *J. Appl. Mech.*, **60**(6), 371-375.
- Civalek, O. (2007), "Nonlinear dynamic response of MDOF systems by the method of harmonic differential quadrature (HDQ)", *Struct. Eng. Mech.*, **25**(2), 201-217.
- Fung, T.C. (2001), Solving initial value problems by differential quadrature method-Part 2: second-and higher-order equations. *Int. J. Numer. Meth. Eng.*, **50**, 1429-1454.
- Fung, T.C. (2002), "Stability and accuracy of differential quadrature method in solving dynamic problems", *Comput. Meth. Appl. Mech. Eng.*, **191**, 1311-1331.
- Gao, Q., Wu, F., Zhang, H.W., Zhong, W.X., Howson, W.P. and Williams, F.W. (2012), "A fast precise integration method for structural dynamics problems", *Struct. Eng. Mech.*, **43**(1), 1-13.
- Goudreau, G.L. and Taylor, R.L. (1972), "Evaluation of numerical integration methods in elasto-dynamics", *Comput. Meth. Appl. Mech. Eng.*, **2**, 69-97.
- Gui, Y., Wang, J.T., Jin, F., Chen, C. and Zhou, M.X. (2014), "Development of a family of explicit algorithms for structural dynamics with unconditional stability", *Nonlin. Dyn.*, **77**(4), 1157-1170.
- Hadianfard, M.A. (2012), "Using integrated displacement method to time-history analysis of steel frames with nonlinear flexible connections", *Struct. Eng. Mech.*, **41**(5), 675-689.
- Hilber, H.M. and Hughes, T.J.R. (1978), "Collocation, dissipation, and 'overshoot' for time integration schemes in structural dynamics", *Earthq. Eng. Struct. Dyn.*, **6**, 99-118.
- Hilber, H.M., Hughes, T.J.R. and Taylor, R.L. (1977), "Improved numerical dissipation for time integration algorithms in structural dynamics", *Earthq. Eng. Struct. Dyn.*, **5**, 283-292.
- Kolay, C. and Ricles, J. (2016), "Assessment of explicit and semi-explicit classes of model-based algorithms for direct integration in structural dynamics", *Int. J. Numer. Meth. Eng.*, **107**, 49-73.
- Kolay, C. and Ricles, J.M. (2014), "Development of a family of unconditionally stable explicit direct integration algorithms with controllable numerical energy dissipation", *Earthq. Eng. Struct. Dyn.*, **43**, 1361-1380.
- Krenk, S. (2008), "Extended state-space time integration with high-frequency energy dissipation", *Int. J. Numer. Meth. Eng.*, **73**, 1767-1787.
- Mohammadzadeh, S., Ghassemieh, M. and Park, Y. (2017), "Structure-dependent improved Wilson- θ method with higher order of accuracy and controllable amplitude decay", *Appl. Math. Model.*, **52**, 417-436.
- Newmark, N.M. (1959), "A method of computation for structural dynamics", *J. Eng. Mech. Div.*, ASCE, **85**, 67-94.
- Penzien, J. (2004), "Dynamic analysis of structure/foundation systems", *Struct. Eng. Mech.*, **17**(3), 281-290.
- Su, C. and Xu, R. (2014), "Random vibration analysis of structures by a time-domain explicit formulation method", *Struct. Eng. Mech.*, **52**(2), 239-260.
- Tang, Y. and Lou, M.L. (2017), "New unconditionally stable explicit integration algorithm for real-time hybrid testing", *J. Eng. Mech.*, **143**(7), 04017029-1-15.
- Wilson, E.L. (1968), "A computer program for the dynamic stress analysis of underground structures", SESM Report No.68-1, Division of Structural Engineering Structural Mechanics, University of California, Berkeley, USA.
- Wood, W.L., Bossak, M. and Zienkiewicz, O.C. (1981), "An alpha modification of Newmark's method", *Int. J. Numer. Meth. Eng.*, **15**, 1562-1566.